

Sampled Softmax with Random Fourier Features

Ankit Singh Rawat, Jiecao Chen, Felix Yu, Ananda Theertha Suresh, and Sanjiv Kumar

Google Research
New York, NY 10011

{ankitsrawat, chenjiecao, felixyu, theertha, sanjivk}@google.com.

July 26, 2019

Abstract

The computational cost of training with softmax cross entropy loss grows linearly with the number of classes. For the settings where a large number of classes are involved, a common method to speed up training is to sample a subset of classes and utilize an estimate of the gradient based on these classes, known as the *sampled softmax* method. However, the sampled softmax provides a biased estimate of the gradient unless the samples are drawn from the exact softmax distribution, which is again expensive to compute. Therefore, a widely employed practical approach (without theoretical justification) involves sampling from a simpler distribution in the hope of approximating the exact softmax distribution. In this paper, we develop the first theoretical understanding of the role that different sampling distributions play in determining the quality of sampled softmax. Motivated by our analysis and the work on kernel-based sampling, we propose the *Random Fourier Softmax* (RF-softmax) method that utilizes the powerful Random Fourier features to enable more efficient and accurate sampling from the (approximate) softmax distribution. We show that RF-softmax leads to low bias in estimation in terms of both the full softmax distribution and the full softmax gradient. Furthermore, the cost of RF-softmax scales only logarithmically with the number of classes.

1 Introduction

The cross entropy loss based on softmax function is widely used in multi-class classification tasks such as natural language processing [1], image classification [2], and recommendation systems [3]. In multi-class classification, given an input $\mathbf{x} \in \mathcal{X}$, the goal is to predict the output class $t \in \{1, 2, \dots, n\}$, where n is the number of classes. Given an input feature \mathbf{x} , the model (often a neural network) first computes an input embedding $\mathbf{h} \in \mathbb{R}^d$ and then the raw scores or *logits* for classes $\mathbf{o} = (o_1, \dots, o_n)$ as the product of the input embedding \mathbf{h} and the class embedding $\mathbf{c}_1, \dots, \mathbf{c}_n \in \mathbb{R}^d$,

$$o_i = \tau \mathbf{h}^T \mathbf{c}_i, \quad (1)$$

where τ is often referred to as the (inverse) *temperature* parameter of softmax. The probability that the model assigns to the i -th class is computed using the *full softmax* function

$$p_i = \frac{e^{o_i}}{Z}, \quad (2)$$

where $Z = \sum_{i=1}^n e^{o_i}$ is called the *partition function*. The distribution in (2) is commonly referred to as the softmax distribution. Given a collection of inputs and their true labels, the objective is to

identify the model parameters by minimizing the *cross-entropy loss* based on softmax function or the *full softmax loss*

$$\mathcal{L} = -\log p_t = -o_t + \log Z, \quad (3)$$

where $t \in [n]$ denotes the true label (class) for the input \mathbf{x}^1 .

First order optimization methods are typically used to train neural network models. This requires computing the gradient of the loss with respect to the model parameter $\boldsymbol{\theta}$ during each iteration

$$\nabla_{\boldsymbol{\theta}} \mathcal{L} = -\nabla_{\boldsymbol{\theta}} o_t + \sum_{i=1}^n \frac{e^{o_i}}{Z} \cdot \nabla_{\boldsymbol{\theta}} o_i = -\nabla_{\boldsymbol{\theta}} o_t + \mathbb{E}_{s \sim p} [\nabla_{\boldsymbol{\theta}} o_s], \quad (4)$$

where the expectation is taken over the softmax distribution (cf. (2)). As evident from (4), computing the gradient of the full softmax loss takes $\mathcal{O}(dn)$ time due to the contributions from all n classes. Therefore, training a model using the full softmax loss becomes prohibitively expensive in the settings where a large number of classes are involved. To this end, various approaches have been proposed for efficient training. This includes different modified loss functions: hierarchical softmax [5] partitions the classes into a tree based on label similarities, allowing for $\mathcal{O}(d \log n)$ training and inference time; spherical softmax [6, 7] replaces the exponential function by a quadratic function, enabling efficient algorithm to compute the updates of the output weights irrespective of the output size. Efficient implementations of softmax on different hardware is also being actively studied [8].

1.1 Sampled softmax

A popular approach to speed up the training of full softmax loss is using *sampled softmax*: instead of including all classes during each iteration, a small random subset of n classes is considered, where each *negative* class is sampled with some probability. Formally, let the number of sampled classes during each iterations be m , with class i being picked with probability q_i . Let $\mathcal{N}_t \triangleq [n] \setminus \{t\}$ be the set of negative classes. Assuming that $s_1, \dots, s_m \in \mathcal{N}_t$ denote the sampled class indices, following [9], we define the adjusted logits $\mathbf{o}' = \{o'_1, o'_2, \dots, o'_{m+1}\}$ such that $o'_1 = o_t$ and for $i \in [m]$,

$$o'_{i+1} = o_{s_i} - \log(mq_{s_i}). \quad (5)$$

Accordingly, we define the *sampled softmax distribution* as $p'_i = \frac{e^{o'_i}}{Z'}$, where $Z' = \sum_{j=1}^{m+1} e^{o'_j}$. Now, the *sampled softmax loss* corresponds to the cross entropy loss with respect to the sampled softmax distribution:

$$\mathcal{L}' = -\log p'_t = -o_t + \log Z'. \quad (6)$$

Since the above loss depends only on $m + 1$ classes, the computational cost is reduced from $\mathcal{O}(dn)$ to $\mathcal{O}(dm)$ as compare to the full softmax loss in (3).

In order for the sampled softmax approach to converge to the same solution, one would like the gradient of the sampled softmax loss to be an unbiased estimator of the gradient of the full softmax loss, i.e.,

$$\mathbb{E} [\nabla_{\boldsymbol{\theta}} \mathcal{L}'] = \nabla_{\boldsymbol{\theta}} \mathcal{L}, \quad (7)$$

where the expectation is taken over the sampling distribution q . As it turns out, the sampling distribution plays a crucial role in ensuring the unbiasedness of $\nabla_{\boldsymbol{\theta}} \mathcal{L}'$. Bengio and Senécal [9] show

¹The results of this paper can be generalized to a multi-label setting, using multi-label to multi-class reductions [4].

that (7) holds if the sampling distribution q is the full softmax distribution itself, i.e., $q_i = p_i \propto e^{o_i}$ in (2).

However, sampling from the softmax distribution itself is again computationally expensive: one needs to compute the partition function Z during each iteration, which is again an $\mathcal{O}(dn)$ operation since Z depends on both current model parameter and input. As a feasible alternative, one usually samples from a distribution which does not depend on the current model parameter and input. Common choices are uniform, log-uniform, or the global prior of classes [10, 1]. However, since these distributions are far from the full softmax distribution, they can lead to significantly worse solutions. Various approaches have been proposed to improve negative sampling. For example, a separate model can be used to track the distribution of softmax in language modeling tasks [9]. One can also use an LSH algorithm to find the approximate nearest classes in the embedding space which in turn helps in sampling from the softmax distribution efficiently [11]. Quadratic kernel softmax [12] uses a kernel-based sampling method and quadratic approximation of the softmax function to draw one sample in sublinear time. Similarly, the Gumbel trick was proposed to sample from the softmax distribution in sublinear time [13]. The partition function can also be written in a double-sum formulation to enable an unbiased sampling algorithm for SGD [14, 15]. Among other training approaches based on sampled losses, Noise Contrastive Estimation (NCE) and its variants avoid computing the partition function [16], and (semi-)hard negative sampling [17, 4, 18] selects the negatives that most violate the current objective function.

1.2 Our contributions

Theory. Despite the large body of work on improving the quality of sampled softmax, developing a theoretical understanding of the performance of sampled softmax has not received much attention. Blanc and Steffen [12] show that the full softmax distribution is the only distribution that provides an unbiased estimate of the true gradient $\nabla_{\theta}\mathcal{L}$. However, it is not clear *how different sampling distributions affects the bias* $\nabla_{\theta}\mathcal{L} - \mathbb{E}[\nabla_{\theta}\mathcal{L}']$. In this paper, we address this issue and characterize the bias of the gradient for a generic sampling distribution (cf. Section 2).

Algorithm. Guided by our analysis and recognizing the practical appeal of kernel-based sampling [12], we propose a new kernel-based sampling method, namely Random Fourier softmax (RF-softmax), in Section 3. RF-softmax employs the powerful Random Fourier features [19] and guarantees small bias of the gradient estimate. Furthermore, the complexity of sampling one class for RF-softmax is $\mathcal{O}(D \log n)$, where D denotes the number of random features used to define the RF-softmax method. In contrast with this, the full softmax and the prior kernel-based sampling method Quadratic-softmax [12] incur $\mathcal{O}(dn)$ and $\mathcal{O}(d^2 \log n)$ computational cost to generate one sample, respectively. Here, d denotes the embedding dimension. In practice, D can be two orders of magnitudes smaller than d^2 to achieve similar or better performance. As a result, RF-softmax method has two desirable features: 1) better accuracy due to small bias and 2) computational efficiency due to low sampling cost.

Experiments. We conduct experiments on widely used NLP and multi-class classification datasets to demonstrate the utility of the proposed RF-softmax method (cf. Section 4).

2 Gradient bias of sampled softmax

The goal of sampled softmax is to obtain a computationally efficient estimate of the *true gradient* $\nabla_{\theta}\mathcal{L}$ (cf. (4)) of the full softmax loss (cf. (3)) with small bias. Arguably ensuring small bias is more

important than ensuring small variance as the large variance has relatively less adverse effects on the final quality of the trained model. In this section we develop a theoretical understanding of how different sampling distributions affect the bias of gradient. To the best of our knowledge, this is the first result of this kind.

For the cross entropy loss based on the sampled softmax (cf. (6)), the training algorithm employs the following estimate of $\nabla_{\theta}\mathcal{L}$.

$$\nabla_{\theta}\mathcal{L}' = -\nabla_{\theta}o_t + \frac{e^{o_t}\nabla_{\theta}o_t + \sum_{i \in [m]} \frac{e^{o_{s_i}}}{mq_{s_i}} \nabla_{\theta}o_{s_i}}{e^{o_t} + \sum_{i \in [m]} \frac{e^{o_{s_i}}}{mq_{s_i}}}. \quad (8)$$

The following result bounds the bias of the estimate $\nabla_{\theta}\mathcal{L}'$. Without loss of generality, we work with the sampling distributions with support \mathcal{N}_t (the set of negative classes), i.e., $q_i > 0$ for each $i \in \mathcal{N}_t$.

Theorem 1. *Let $\nabla_{\theta}\mathcal{L}'$ (cf. (8)) be the estimate of $\nabla_{\theta}\mathcal{L}$ based on m negative classes s_1, \dots, s_m , drawn according to the sampling distribution q . We further assume that the gradients of the logits $\nabla_{\theta}o_i$ have their coordinates bounded² by M . Then, the bias of $\nabla_{\theta}\mathcal{L}'$ satisfies*

$$\text{LB} \leq \mathbb{E} [\nabla_{\theta}\mathcal{L}'] - \nabla_{\theta}\mathcal{L} \leq \text{UB} \quad (9)$$

with

$$\begin{aligned} \text{LB} &\triangleq -\frac{M \sum_{k \in \mathcal{N}_t} e^{o_k} \left| Z_t - \frac{e^{o_k}}{q_k} \right|}{mZ^2} \left(1 - o\left(\frac{1}{m}\right) \right) \cdot \mathbf{1}, \\ \text{UB} &\triangleq \underbrace{\left(\frac{\sum_{j \in \mathcal{N}_t} \frac{e^{2o_j}}{q_j} - Z_t^2}{mZ^3} + o\left(\frac{1}{m}\right) \right)}_{\text{UB}_1} \cdot \mathbf{g} + \underbrace{\left(\frac{2M}{m} \frac{\max_{i, i' \in \mathcal{N}_t} \left| \frac{e^{o_i}}{q_i} - \frac{e^{o_{i'}}}{q_{i'}} \right| Z_t}{Z^2 + \sum_{j \in \mathcal{N}_t} \frac{e^{2o_j}}{q_j}} + o\left(\frac{1}{m}\right) \right)}_{\text{UB}_2} \cdot \mathbf{1}, \end{aligned} \quad (10)$$

where $Z_t \triangleq \sum_{j \in \mathcal{N}_t} e^{o_j}$, $\mathbf{g} \triangleq \sum_{j \in \mathcal{N}_t} e^{o_j} \nabla_{\theta}o_j$ and $\mathbf{1}$ is the all one vector.

The proof of Theorem 1 is presented in the appendix.

Theorem 1 captures the effect of the underlying sampling distribution q on the bias of gradient estimate in terms of three (closely related) quantities:

$$\sum_{j \in \mathcal{N}_t} \frac{e^{2o_j}}{q_j}, \quad \max_{j, j' \in \mathcal{N}_t} \left| \frac{e^{o_j}}{q_j} - \frac{e^{o_{j'}}}{q_{j'}} \right|, \quad \text{and} \quad \left| \sum_{j \in \mathcal{N}_t} e^{o_j} - \frac{e^{o_k}}{q_k} \right|.$$

Ideally, we would like to pick a sampling distribution for which all these quantities are as small as possible. Since q is a probability distribution, it follows from Cauchy-Schwarz inequality that

$$\sum_j \frac{e^{2o_j}}{q_j} = \left(\sum_j q_j \right) \cdot \left(\sum_j \frac{e^{2o_j}}{q_j} \right) \geq \left(\sum_j e^{o_j} \right)^2. \quad (11)$$

If $q_j \propto e^{o_j}$, then (11) is attained (equivalently, $\sum_j \frac{e^{2o_j}}{q_j}$ is minimized). In particular, this implies that UB_1 in (10) disappears. Furthermore, for such distribution we have $q_j = \frac{e^{o_j}}{\sum_{i \in \mathcal{N}_t} e^{o_i}}$. This implies that both UB_2 and LB disappear for such a distribution as well. This guarantees a small bias of the gradient estimate $\nabla_{\theta}\mathcal{L}$. Since sampling from this distribution is computationally expensive, the discussion above suggests that for LB and UB to be simultaneously small, q_j should provide a tight *uniform multiplicative approximation* of e^{o_j} .

²This assumption naturally holds in most of the practical implementations, where each of the gradient coordinates or norm of the gradient is clipped by a threshold.

Method	Quadratic [12]	Random Fourier [19]			Random Maclaurin [20]
Dimension	$D = 256^2$	$D = 100$	$D = 1000$	$D = 256^2$	$D = 256^2$
MSE	2.8e-3	2.6e-3	2.7e-4	5.5e-6	8.8e-2

Table 1: Mean squared error (MSE) of approximating a kernel $\exp(\tau \mathbf{h}^T \mathbf{c})$. \mathbf{h} and \mathbf{c} are randomly sampled from the USPS dataset ($d = 256$). The data is normalized $\|\mathbf{h}\|_2 = 1$, $\|\mathbf{c}\|_2 = 1$ and $1/\sqrt{\tau} = 0.3$ (same setting in the experiment section). For Quadratic, we assume the form is $\alpha \cdot (\mathbf{h}^T \mathbf{c}_i)^2 + \beta$ and solve α and β in a linear system to get the optimal MSE. In practice, with fixed α and β as in [12], the MSE will be larger. Random Fourier has much lower MSE with same D , and much smaller D with similar MSE. Also note that Random Fourier and Random Maclaurin are unbiased.

3 Random Fourier Softmax (RF-Softmax)

In this section, guided by the conclusion in Section 2, we propose Random Fourier Softmax (RF-softmax), as a new sampling method that employs Random Fourier features to tightly approximate the full softmax distribution. RF-softmax falls under the broader class of kernel-based sampling methods which are amenable to efficient implementation. Before presenting RF-softmax, we briefly describe the kernel-based sampling and an existing method based quadratic kernels [12].

3.1 Kernel-based sampling and Quadratic-softmax

Given a kernel $K : \mathbb{R}^d \times \mathbb{R}^d \rightarrow \mathbb{R}$, the input embedding $\mathbf{h} \in \mathbb{R}^d$, and the class embeddings $\mathbf{c}_1, \dots, \mathbf{c}_n \in \mathbb{R}^d$, kernel-based sampling selects the class i with probability $q_i = \frac{K(\mathbf{h}, \mathbf{c}_i)}{\sum_{j=1}^n K(\mathbf{h}, \mathbf{c}_j)}$. Note that if $K(\mathbf{h}, \mathbf{c}_i) = \exp(o_i) = \exp(\tau \mathbf{h}^T \mathbf{c}_i)$, this amounts to directly sampling from the softmax distribution as we have $q_i = p_i$.

Blanc and Steffen [12] show that if the kernel can be linearized by a mapping $\phi : \mathbb{R}^d \rightarrow \mathbb{R}^D$ such that $K(\mathbf{h}, \mathbf{c}_i) = \phi(\mathbf{h})^T \phi(\mathbf{c}_i)$, sampling one point from the distribution takes only $\mathcal{O}(D \log n)$ time by a divide-and-conquer algorithm. Based on the above they further propose a sampled softmax approach which utilizes the quadratic kernel to define the sampling distribution.

$$K_{quad}(\mathbf{h}, \mathbf{c}_i) = \alpha \cdot (\mathbf{h}^T \mathbf{c}_i)^2 + 1. \quad (12)$$

Note that the quadratic kernel can be linearized by the mapping $\phi(\mathbf{z}) = [\sqrt{\alpha} \cdot (\mathbf{z} \otimes \mathbf{z}), 1]$. This implies that $D = \mathcal{O}(d^2)$; consequently, sampling one class takes $\mathcal{O}(d^2 \log n)$ time. Despite the promising results of Quadratic-softmax, it has the following caveats.

- The quadratic function (c.f. (12) with $\alpha = 100$, the value used in [12]) does not give a tight multiplication approximation of the exponential kernel e^{o_j} . According to the analysis in Section 2, this results in a gradient estimate with large bias.
- The $\mathcal{O}(d^2)$ computational cost can be prohibitive for models with large embedding dimensions.
- Since a quadratic function is a poor approximation of the exponential function for negative numbers, it is used to approximate a modified *absolute softmax* loss function in [12] instead, where *absolute* values of logits serve as input to the softmax function.

Next, we present a novel kernel-based sampling method that addresses all of these shortcomings.

3.2 RF-softmax

Given the analysis in Section 2 and low computational cost of the kernel-based sampling methods defined by linearizable kernels, our goal is to come up with a linearizable kernel (better than quadratic) that provides a good uniform multiplicative approximation of the exponential kernel $K(\mathbf{h}, \mathbf{c}) = e^o = e^{\tau \mathbf{h}^T \mathbf{c}}$. More concretely, we would like to find a nonlinear map $\phi(\cdot) : \mathbb{R}^d \rightarrow \mathbb{R}^D$ such that the error between $K(\mathbf{h}, \mathbf{c})$ and $\hat{K}(\mathbf{h}, \mathbf{c}) = \phi(\mathbf{h})^T \phi(\mathbf{c})$ is small, for all values of \mathbf{h} and \mathbf{c} .

The random Maclaurin features [20] seem to be an obvious choice here since it provides an unbiased estimator of the exponential kernel. However, due to rank deficiency of the produced features, it requires large dimensions D in order to achieve small mean squared error [21, 22]. We verify that this is indeed not a good choice in Table 1.

In contrast, the Random Fourier features (RFF) [19] is much more compact [21]. Moreover, these features are also better theoretically understood [23], with significant efforts focusing on the improving the efficiency and quality (see, e.g., [24, 25]). This leads to the natural questions: *Can we use RFF to approximate the exponential kernel?* However, this approach faces a major challenge at the outset: RFF only works for positive definite shift-invariant kernels such as the Gaussian kernel, while the exponential kernel is not shift-invariant.

A key observation is that when the input embedding \mathbf{h} and class embedding \mathbf{c} are normalized, the exponential kernel becomes the Gaussian kernel (up to a multiplicative constant):

$$e^{\tau \mathbf{h}^T \mathbf{c}} = e^\tau e^{-\frac{\tau \|\mathbf{h} - \mathbf{c}\|_2^2}{2}}. \quad (13)$$

The normalization does not hurt the expressive power of softmax as it only loses one degree of freedom. In fact, normalized embeddings are widely used in practice to improve training stability and model quality [26, 27, 28]. In particular, it attains improved performance as long as τ (cf. (1)) is large enough to ensure that the output of softmax can cover (almost) the entire range $(0, 1)^3$.

Remark 1. *Due to the quality improvement and the quest to apply RFF, we focus on the settings where both the class embeddings \mathbf{c}_i and input embeddings \mathbf{h} are ℓ_2 normalized.*

For the Gaussian kernel $K(\mathbf{x} - \mathbf{y}) = e^{-\frac{\nu \|\mathbf{x} - \mathbf{y}\|^2}{2}}$ with temperature parameter ν , the D -dimensional RFF map takes the following form.

$$\phi_{\frac{1}{\sqrt{\nu}}, D}(\mathbf{u}) = \frac{1}{\sqrt{D}} \left[\cos(\mathbf{w}_1^T \mathbf{u}), \dots, \cos(\mathbf{w}_D^T \mathbf{u}), \sin(\mathbf{w}_1^T \mathbf{u}), \dots, \sin(\mathbf{w}_D^T \mathbf{u}) \right], \quad (14)$$

where $\mathbf{w}_1, \dots, \mathbf{w}_D \sim N(0, \mathbf{I}/\nu)$. The RFF map provides an unbiased approximation of Gaussian kernel

$$e^{-\frac{\nu \|\mathbf{x} - \mathbf{y}\|^2}{2}} \approx \phi_{\frac{1}{\sqrt{\nu}}, D}(\mathbf{x})^T \phi_{\frac{1}{\sqrt{\nu}}, D}(\mathbf{y}). \quad (15)$$

Now, given input embedding \mathbf{h} , if we sample class i with probability $q_i \propto \exp(-\tau \|\mathbf{c}_i - \mathbf{h}\|^2/2)$, then it follows from (13) (set $\nu = \tau$, $\mathbf{x} = \mathbf{c}_i$, $\mathbf{y} = \mathbf{h}$) that our sampling distribution is the same as the softmax distribution. Therefore, with normalized embeddings, one can employ the kernel-based sampling to realize the sampled softmax such that class i is sampled with the probability

$$q_i \propto \phi_{\frac{1}{\sqrt{\nu}}, D}(\mathbf{c}_i)^T \phi_{\frac{1}{\sqrt{\nu}}, D}(\mathbf{h}). \quad (16)$$

³In Section 4, we verify that restriction to the normalized embedding does not hurt and in fact improves the final performance.

We refer to this method as Random Fourier softmax (RF-softmax). RF-softmax costs $\mathcal{O}(D \log n)$ to sample one point. Note that computing the nonlinear map takes $\mathcal{O}(Dd)$ time with the classic Random Fourier feature. One can easily use the structured orthogonal random feature (SORF) technique [24] to reduce this complexity to $\mathcal{O}(D \log d)$ with even lower approximation error. Since typically the embedding dimension d is on the order of hundreds and we consider large n : $d \ll n$, the overall complexity of RF-softmax is $\mathcal{O}(D \log n)$.

As shown in Table 1, the RFF map approximates the exponential kernel with the mean squared error with the same mapping dimension D (or the mapping dimensions D with same mean squared error) which is orders of magnitudes smaller than that for the quadratic map. Recall that quadratic map defines the state of the art kernel-based sampling Quadratic-softmax (cf. Section 3.1).

Even though the use of RFF looks straightforward for normalized embeddings, it raises interesting implementation related challenges in terms of selecting the temperature parameter ν to realize low biased sampling. We address this challenge in the next section.

3.3 Analysis and discussions

Recall that the discussion following Theorem 1 implies that, for the low biased gradient estimates, the sampling distribution q_i needs to form a tight multiplicative approximation of the softmax distribution p_i , where $p_i \propto \exp(o_i) = \exp(\tau \mathbf{h}^T \mathbf{c}_i)$. In the following result, we quantify the quality of the proposed RF-softmax based on the ratio $|p_i/q_i|$. The proof is presented in the appendix.

Theorem 2. *Given the ℓ_2 -normalized input embedding \mathbf{h} and ℓ_2 -normalized class embeddings $\{\mathbf{c}_1, \dots, \mathbf{c}_n\}$, let $o_i = \tau \mathbf{h}^T \mathbf{c}_i$ be the logits associated with the class i . Let q_i denote the probability of sampling the i -th class based on D -dimensional Random Fourier features, i.e., $q_i = \frac{1}{C} \cdot \phi_{\frac{1}{\sqrt{\nu}}, D}(\mathbf{c}_i)^T \phi_{\frac{1}{\sqrt{\nu}}, D}(\mathbf{h})$, where C is the normalizing constant. Then, as long as $e^{2\nu} \leq \frac{\gamma_1}{\rho \sqrt{d}} \cdot \frac{\sqrt{D}}{\log D}$, the following holds with probability at least $1 - \mathcal{O}\left(\frac{1}{D^2}\right)$.*

$$e^{(\tau-\nu)\mathbf{h}^T \mathbf{c}_i} \cdot (1 - \gamma_2) \leq \frac{1}{\sum_{i \in \mathcal{N}_t} e^{o_i}} \cdot \left| \frac{e^{o_i}}{q_i} \right| \leq e^{(\tau-\nu)\mathbf{h}^T \mathbf{c}_i} \cdot (1 + \gamma_2), \quad (17)$$

where γ_1, γ_2 , and ρ are positive constants.

Remark 2. *With large enough D such that $e^{2\tau} \leq \frac{\gamma_1}{\rho \sqrt{d}} \cdot \frac{\sqrt{D}}{\log D}$, as per Theorem 2, one can select $\nu = \tau$, which ensures that $q_i \propto (1 \pm o_D(1)) \cdot p_i \quad \forall i \in \mathcal{N}_t$. In particular, at $D = \infty$, we have $q_i \propto p_i$.*

Note that Theorem 2 and Remark 2 highlight an important design issue in the implementation of the RF-softmax approach. The ability of q to approximate p (as stated in (17)) degrades as the difference $|\tau - \nu|$ increases. Therefore, one would like to pick ν to be as close to τ as possible (ideally exactly equal to τ). However, for the fixed dimension of the feature map D , the approximation guarantee in (17) holds for only those values of ν that are bounded by a function of D . Therefore, the dimension of the Random Fourier feature map D dictates which Gaussian kernels we can utilize in the proposed RF-softmax approach. On the other hand, the variance of the kernel approximation of Random Fourier feature grows with ν [24]. Additionally, in order to work with the normalized embeddings, it's necessary to select a reasonably large value for the temperature parameter τ^4 . Therefore, choosing $\nu = \tau$ in this case will result in larger variance of the estimated kernel.

Remark 3. *As a trade off between bias and variance on approximating the exponential kernel, with a limited D and large τ , ν should be set as a value smaller than τ .*

⁴This provides a wide enough range for the logits values; thus, ensuring the underlying model has sufficient expressive power. The typical choice ranges from 5 to 30.

In Section 4, we explore different choices for the value of ν and confirm that some $\nu < \tau$ achieves the best empirical performance.

4 Experiments

To verify the proposed sampling method and theoretical analysis, we experimentally evaluate the proposed RF-softmax and compare it with several baselines with simple neural networks. Though with much lower computational cost, on the final model quality, RF-softmax ($\mathcal{O}(D \log n)$, $D \ll d^2$) performs at par with the sampled softmax approach based on the full softmax distribution ($\mathcal{O}(dn)$), and it outperforms Quadratic-softmax [12] that uses the quadratic function to approximate the exponential kernel ($\mathcal{O}(d^2 \log n)$). In addition, we highlight the effect of the different design choices regarding the underlying RFF map $\phi_{\frac{1}{\sqrt{\nu}}, D}$ (cf. (14)) on the final performance of RF-softmax.

4.1 Datasets and models

NLP datasets. PENNTREEBANK [29] is a popular benchmark for NLP tasks with a vocabulary of size 10,000. We train a language model using LSTM, where the normalized output of the LSTM serves as the input embedding. BNEWS [30] is another NLP dataset. We select the most frequent 64,000 words as the vocabulary. Our model architecture for BNEWS is the same as the one used for PENNTREEBANK with more parameters. The embedding dimension $d = 200$ for PENNTREEBANK and $d = 512$ for BNEWS.

Extreme classification datasets. We test the proposed method on three classification datasets with large number of classes [31]. For each data point of v -dimensional (sparse) feature, a $v \times 128$ matrix with normalized rows is first applied to map it to a 128-dimensional vector ($d = 128$). Once normalized, this vector serves as the input embedding \mathbf{h} . For $i \in [n]$, class i is mapped to a 128-dimensional normalized vector \mathbf{c}_i . Following the convention of extreme classification literature, we report precision at k (PREC@K) on the test set.

Recall that the proposed RF-softmax draws samples with computational complexity $\mathcal{O}(D \log n)$. We compare it with the following baselines.

- FULL, the full softmax loss (cf. (3)), which has computational complexity $\mathcal{O}(dn)$.
- EXP, the sampled softmax approach with the full softmax distribution (cf. (2)) as the sampling distribution. This again has computational complexity $\mathcal{O}(dn)$ to draw one sample.
- UNIFORM, the sampled softmax approach that draws negative classes uniformly at random, amounting to $\mathcal{O}(1)$ computational complexity to draw one sample.
- QUADRATIC, the sampled softmax approach based on a quadratic kernel (cf. (12)). We follow the implementation of [12] and use $\alpha o^2 + 1$ with $\alpha = 100$. Since $\alpha o^2 + 1$ is a better approximation of $e^{|o|}$ than it is of e^o , [12] propose to use the absolute softmax function $\tilde{p}_i = \frac{e^{\sigma|o_i|}}{\sum_{j \in [n]} e^{\sigma|o_j|}}$ while computing the cross entropy loss. We employ this modified loss function for the quadratic kernel as it gives better results as compared to full softmax loss in (3). The cost of drawing one sample with this method is $\mathcal{O}(d^2 \log n)$.

In this section, we call $T = 1/\sqrt{\tau}$ the temperature of softmax (cf. (2)). We set this parameter to 0.3 as it leads to the best performance for the FULL baseline. This is a natural choice given that sampled softmax aims at approximating this loss function with a small subset of (sampled) negative classes.

# classes (n)	Method	Wall time
10,000	EXP	1.4 ms
	QUADRATIC	6.5 ms
	RFF ($D = 50$)	0.5 ms
	RFF ($D = 200$)	0.6 ms
	RFF ($D = 500$)	1.2 ms
	RFF ($D = 1,000$)	1.4 ms
500,000	EXP	32.3 ms
	QUADRATIC	8.2 ms
	RFF ($D = 50$)	1.6 ms
	RFF ($D = 200$)	1.7 ms
	RFF ($D = 500$)	2.0 ms
	RFF ($D = 1,000$)	2.4 ms

Table 2: Wall time of model dependent sampling methods. ($m = 10$ and embedding dimension $d = 64$.)

4.2 Experimental results

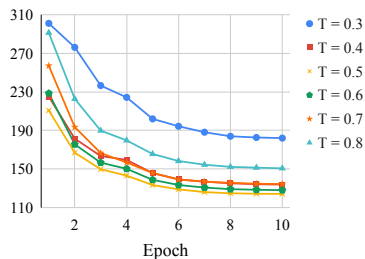


Figure 1: Validation perplexity for RF-softmax on PENNTREEBANK with $m = 100$, $D = 1024$ and varying values of T .

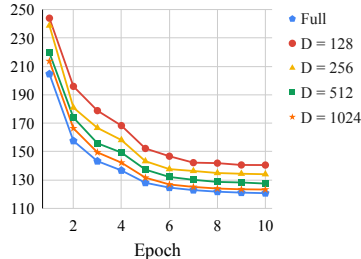


Figure 2: Validation perplexity for RF-softmax on PENNTREEBANK with $m = 100$ and varying D .

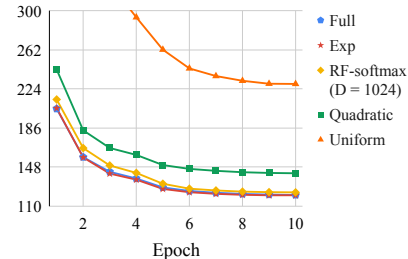


Figure 3: Comparison of RF-softmax with other baselines on PENNTREEBANK when $m = 100$.

Wall time. We begin with verifying that the RF-softmax indeed incurs low sampling cost. In Table 2, we compare the wall-time that different (model dependent) sampling methods take to compute the sampled softmax loss (cf. (6)) for different sets of parameters.

Normalized vs. unnormalized embeddings. To justify our choice of working with normalized embeddings, we ran experiments for FULL with and without embedding normalization for both PENNTREEBANK and AMAZONCAT-13K. On PENNTREEBANK, after 10 epochs, the unnormalized version has validation perplexity 126 as compared to 120 with the normalized version (smaller is better). On AMAZONCAT-13K, both versions have PREC@1 87%. Next, we discuss the key design choices for RF-softmax: the choice of the Gaussian sampling kernel defined by ν (cf. (13)); and the dimension of the Random Fourier feature map D .

Effect of the parameter ν . As discussed in Section 3.2, for a finite D , we should choose $\nu < \sigma$ as a trade off between the variance and bias. Figure 1 shows the performance of the proposed RF-softmax method on PENNTREEBANK for different values of ν . In particular, we vary $T = \frac{1}{\sqrt{\nu}}$ as it defines the underlying Random Fourier feature map (cf. (15)). The best performance is attained at $T = 0.5$. This choice of $\nu < \sigma$ is in line with our discussion in Section 3.3. We use this same setting in all other experiments.

Dataset	Method	PREC@1	PREC@3	PREC@5
AMAZONCAT-13K $n = 13,330$ $v = 203,882$	EXP	0.87	0.76	0.62
	UNIFORM	0.83	0.69	0.55
	QUADRATIC	0.84	0.74	0.60
	RFF	0.87	0.75	0.61
DELICIOUS-200K $n = 205,443$ $v = 782,585$	EXP	0.42	0.38	0.37
	UNIFORM	0.36	0.34	0.32
	QUADRATIC	0.40	0.36	0.34
	RFF	0.41	0.37	0.36
WIKILSHTC $n = 325,056$ $v = 1,617,899$	EXP	0.58	0.37	0.29
	UNIFORM	0.47	0.29	0.22
	QUADRATIC	0.57	0.37	0.28
	RFF	0.56	0.35	0.26

Table 3: Comparison among sampled softmax methods on extreme classification datasets. We report the metrics based on the same number of training iterations for all methods.

Effect of D . The accuracy of the approximation of the Gaussian kernel using the RFF map improves as we increase the dimension of the map D (cf. (14)). Figure 2 demonstrates the performance of the proposed RF-softmax method on PENNTREEBANK for different values of D . As expected, the performance of RF-softmax gets closer to that of FULL when we increase D .

RF-softmax vs. baselines. Figure 3 illustrates the performance of different sampled softmax approaches on PENNTREEBANK. The figure shows the validation perplexity as the training progresses. As expected, the performance of expensive EXP is very close to the performance of FULL. The RF-softmax method outperforms both QUADRATIC and UNIFORM. We note that RF-softmax with $D = 1024$ performs better than QUADRATIC method with significantly lower computational and space cost. Since we have embedding dimension $d = 200$, RF-softmax is almost 40X more efficient as compared to QUADRATIC (D vs. d^2). Figure 4 shows the performance on the BNEWS dataset. Performance of RF-softmax is at par with QUADRATIC with $D = 2048$ and outperforms QUADRATIC with $D = 8192$. In this experiment, we have $d = 512$, so RF-softmax with $D = 2048$ and $D = 8192$ are 128X and 32X more efficient than QUADRATIC, respectively.

Table 3 shows the performance of various sampling methods on three extreme classification datasets [31]. We do not report PREC@K values for FULL as the performance of EXP is an accurate proxy for those. The results demonstrate that RF-softmax attains better/comparable performance relative to QUADRATIC. For WIKILSHTC, even though QUADRATIC has better PREC@K values, RF-softmax leads to 4% smaller full softmax loss, and this verifies our analysis.

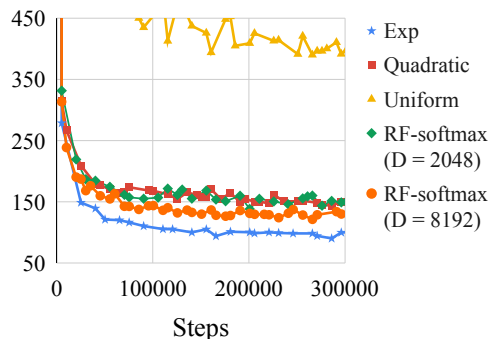


Figure 4: Comparison of RF-softmax with other baselines on BNEWS with $m = 100$.

References

- [1] Tomas Mikolov, Ilya Sutskever, Kai Chen, Greg S Corrado, and Jeff Dean. Distributed representations of words and phrases and their compositionality. In *Advances in Neural Information Processing Systems*, pages 3111–3119, 2013.
- [2] Alex Krizhevsky, Ilya Sutskever, and Geoffrey E Hinton. Imagenet classification with deep convolutional neural networks. In *Advances in Neural Information Processing Systems*, pages 1097–1105, 2012.
- [3] Paul Covington, Jay Adams, and Emre Sargin. Deep neural networks for youtube recommendations. In *Proceedings of the 10th ACM Conference on Recommender Systems*, pages 191–198. ACM, 2016.
- [4] Sashank J Reddi, Satyen Kale, Felix Yu, Dan Holtmann-Rice, Jiecao Chen, and Sanjiv Kumar. Stochastic negative mining for learning with large output spaces. *Proceedings of the International Conference on Artificial Intelligence and Statistics*, 2019.
- [5] Frederic Morin and Yoshua Bengio. Hierarchical probabilistic neural network language model. In *Proceedings of the International Conference on Artificial Intelligence and Statistics*, volume 5, pages 246–252, 2005.
- [6] Pascal Vincent, Alexandre De Brébisson, and Xavier Bouthillier. Efficient exact gradient update for training deep networks with very large sparse targets. In *Advances in Neural Information Processing Systems*, pages 1108–1116, 2015.
- [7] Alexandre de Brébisson and Pascal Vincent. An exploration of softmax alternatives belonging to the spherical loss family. *arXiv preprint arXiv:1511.05042*, 2015.
- [8] Edouard Grave, Armand Joulin, Moustapha Cissé, Hervé Jégou, et al. Efficient softmax approximation for gpus. In *Proceedings of the 34th International Conference on Machine Learning*, pages 1302–1310. JMLR. org, 2017.
- [9] Yoshua Bengio and Jean-Sébastien Senécal. Adaptive importance sampling to accelerate training of a neural probabilistic language model. *IEEE Transactions on Neural Networks*, 19(4):713–722, 2008.
- [10] Sébastien Jean, Kyunghyun Cho, Roland Memisevic, and Yoshua Bengio. On using very large target vocabulary for neural machine translation. *arXiv preprint arXiv:1412.2007*, 2014.
- [11] Sudheendra Vijayanarasimhan, Jonathon Shlens, Rajat Monga, and Jay Yagnik. Deep networks with large output spaces. *arXiv preprint arXiv:1412.7479*, 2014.
- [12] Guy Blanc and Steffen Rendle. Adaptive sampled softmax with kernel based sampling. In *International Conference of Machine Learning*, 2018.
- [13] Stephen Mussmann, Daniel Levy, and Stefano Ermon. Fast amortized inference and learning in log-linear models with randomly perturbed nearest neighbor search. *arXiv preprint arXiv:1707.03372*, 2017.
- [14] Parameswaran Raman, Sriram Srinivasan, Shin Matsushima, Xinhua Zhang, Hyokun Yun, and SVN Vishwanathan. DS-MLR: Exploiting double separability for scaling up distributed multinomial logistic regression. *arXiv preprint arXiv:1604.04706*, 2016.
- [15] Francois Fagan and Garud Iyengar. Unbiased scalable softmax optimization. *arXiv preprint arXiv:1803.08577*, 2018.
- [16] Andriy Mnih and Koray Kavukcuoglu. Learning word embeddings efficiently with noise-contrastive estimation. In *Advances in Neural Information Processing Systems*, pages 2265–2273, 2013.
- [17] Florian Schroff, Dmitry Kalenichenko, and James Philbin. Facenet: A unified embedding for face recognition and clustering. In *Proceedings of the IEEE Conference on Computer Vision and Pattern Recognition*, pages 815–823, 2015.
- [18] Ian En-Hsu Yen, Satyen Kale, Felix Yu, Daniel Holtmann-Rice, Sanjiv Kumar, and Pradeep Ravikumar. Loss decomposition for fast learning in large output spaces. In *International Conference on Machine Learning*, pages 5626–5635, 2018.

- [19] Ali Rahimi and Benjamin Recht. Random features for large-scale kernel machines. In *Advances in Neural Information Processing Systems*, pages 1177–1184, 2008.
- [20] Purushottam Kar and Harish Karnick. Random feature maps for dot product kernels. In *Proceedings of the International Conference on Artificial Intelligence and Statistics*, 2012.
- [21] Jeffrey Pennington, Felix Xinnan X Yu, and Sanjiv Kumar. Spherical random features for polynomial kernels. In *Advances in Neural Information Processing Systems*, pages 1846–1854, 2015.
- [22] Raffay Hamid, Ying Xiao, Alex Gittens, and Dennis DeCoste. Compact random feature maps. In *International Conference on Machine Learning*, pages 19–27, 2014.
- [23] Bharath Sriperumbudur and Zoltán Szabó. Optimal rates for random fourier features. In *Advances in Neural Information Processing Systems*, pages 1144–1152, 2015.
- [24] Felix X Yu, Ananda Theertha Suresh, Krzysztof M Choromanski, Daniel N Holtmann-Rice, and Sanjiv Kumar. Orthogonal random features. In *Advances in Neural Information Processing Systems*, pages 1975–1983, 2016.
- [25] Jiyan Yang, Vikas Sindhwani, Haim Avron, and Michael Mahoney. Quasi-Monte Carlo feature maps for shift-invariant kernels. In *International Conference on Machine Learning*, pages 485–493, 2014.
- [26] Rajeev Ranjan, Carlos D Castillo, and Rama Chellappa. L2-constrained softmax loss for discriminative face verification. *arXiv preprint arXiv: 1703.09507*, 2017.
- [27] Weiyang Liu, Yandong Wen, Zhiding Yu, Ming Li, Bhiksha Raj, and Le Song. SpheroFace: Deep hypersphere embedding for face recognition. In *The IEEE Conference on Computer Vision and Pattern Recognition (CVPR)*, volume 1, page 1, 2017.
- [28] Feng Wang, Xiang Xiang, Jian Cheng, and Alan Loddon Yuille. NormFace: 12 hypersphere embedding for face verification. In *Proceedings of the 25th ACM International Conference on Multimedia*, pages 1041–1049. ACM, 2017.
- [29] Mitchell P. Marcus, Beatrice Santorini, Mary Ann Marcinkiewicz, and Ann Taylor. Treebank-3 LDC99T42. 1999.
- [30] David Graff, John S. Garofolo, Jonathan G. Fiscus, William Fisher, and David Pallett. 1996 English broadcast news speech (HUB4) LDC97S44. 1997.
- [31] Manik Varma. Extreme classification repository. Website, 8 2018. <http://manikvarma.org/downloads/XC/XMLRepository.html>.

A Proof of Theorem 1

It follows from (8) that

$$\mathbb{E} [\nabla_{\boldsymbol{\theta}} \mathcal{L}'] = -\nabla_{\boldsymbol{\theta}} o_t + \mathbb{E} \left[\frac{e^{o_t} \cdot \nabla_{\boldsymbol{\theta}} o_t + \sum_{i \in [m]} \left(\frac{e^{o_{s_i}}}{mq_{s_i}} \cdot \nabla_{\boldsymbol{\theta}} o_{s_i} \right)}{e^{o_t} + \sum_{i \in [m]} \frac{e^{o_{s_i}}}{mq_{s_i}}} \right] \quad (18)$$

Let's define random variables

$$U = e^{o_t} \cdot \nabla_{\boldsymbol{\theta}} o_t + \sum_{i \in [m]} \left(\frac{e^{o_{s_i}}}{mq_{s_i}} \cdot \nabla_{\boldsymbol{\theta}} o_{s_i} \right) \quad (19)$$

and

$$V = e^{o_t} + \sum_{i \in [m]} \frac{e^{o_{s_i}}}{mq_{s_i}}. \quad (20)$$

Note that we have

$$\mathbb{E}[U] = \sum_{j \in [n]} e^{o_j} \cdot \nabla_{\boldsymbol{\theta}} o_j \quad \text{and} \quad \mathbb{E}[V] = e^{o_t} + \sum_{j \in \mathcal{N}_t} e^{o_j} = \sum_{j \in [n]} e^{o_j} = Z, \quad (21)$$

Lower bound: It follows from (18) and the lower bound in Lemma 1 that

$$\begin{aligned} \mathbb{E} [\nabla_{\boldsymbol{\theta}} \mathcal{L}'] &\geq -\nabla_{\boldsymbol{\theta}} o_t + \frac{e^{o_t} \cdot \nabla_{\boldsymbol{\theta}} o_t}{\sum_{j \in [n]} e^{o_j}} + \sum_{k \in \mathcal{N}_t} \frac{e^{o_k} \cdot \nabla_{\boldsymbol{\theta}} o_k}{e^{o_t} + \frac{m-1}{m} \cdot \sum_{j \in \mathcal{N}_t} e^{o_j} + \frac{e^{o_k}}{mq_k}} \\ &= -\nabla_{\boldsymbol{\theta}} o_t + \frac{e^{o_t} \cdot \nabla_{\boldsymbol{\theta}} o_t}{\sum_{j \in [n]} e^{o_j}} + \\ &\quad \sum_{k \in \mathcal{N}_t} \frac{e^{o_k} \cdot \nabla_{\boldsymbol{\theta}} o_k}{\sum_{j \in [n]} e^{o_j}} + \left(\sum_{k \in \mathcal{N}_t} \frac{e^{o_k} \cdot \nabla_{\boldsymbol{\theta}} o_k}{e^{o_t} + \frac{m-1}{m} \cdot \sum_{j \in \mathcal{N}_t} e^{o_j} + \frac{e^{o_k}}{mq_k}} - \sum_{k \in \mathcal{N}_t} \frac{e^{o_k} \cdot \nabla_{\boldsymbol{\theta}} o_k}{e^{o_t} + \sum_{j \in \mathcal{N}_t} e^{o_j}} \right) \\ &= -\nabla_{\boldsymbol{\theta}} o_t + \frac{e^{o_t} \cdot \nabla_{\boldsymbol{\theta}} o_t}{\sum_{j \in [n]} e^{o_j}} + \frac{\sum_{k \in \mathcal{N}_t} e^{o_k} \cdot \nabla_{\boldsymbol{\theta}} o_k}{\sum_{j \in [n]} e^{o_j}} + \\ &\quad \frac{1}{m} \sum_{k \in \mathcal{N}_t} \frac{e^{o_k} \cdot \left(\sum_{j \in \mathcal{N}_t} e^{o_j} - \frac{e^{o_k}}{q_k} \right) \cdot \nabla_{\boldsymbol{\theta}} o_k}{\left(e^{o_t} + \frac{m-1}{m} \cdot \sum_{j \in \mathcal{N}_t} e^{o_j} + \frac{e^{o_k}}{mq_k} \right) \left(e^{o_t} + \sum_{j \in \mathcal{N}_t} e^{o_j} \right)} \\ &= \nabla_{\boldsymbol{\theta}} \mathcal{L} + \frac{1}{m} \sum_{k \in \mathcal{N}_t} \frac{e^{o_k} \cdot \left(\sum_{j \in \mathcal{N}_t} e^{o_j} - \frac{e^{o_k}}{q_k} \right) \cdot \nabla_{\boldsymbol{\theta}} o_k}{\left(e^{o_t} + \frac{m-1}{m} \cdot \sum_{j \in \mathcal{N}_t} e^{o_j} + \frac{e^{o_k}}{mq_k} \right) \left(e^{o_t} + \sum_{j \in \mathcal{N}_t} e^{o_j} \right)} \\ &\geq \nabla_{\boldsymbol{\theta}} \mathcal{L} - \frac{1}{m} \sum_{k \in \mathcal{N}_t} \frac{e^{o_k} \cdot \left| \sum_{j \in \mathcal{N}_t} e^{o_j} - \frac{e^{o_k}}{q_k} \right| \cdot |\nabla_{\boldsymbol{\theta}} o_k|}{\left(e^{o_t} + \frac{m-1}{m} \cdot \sum_{j \in \mathcal{N}_t} e^{o_j} + \frac{e^{o_k}}{mq_k} \right) \left(e^{o_t} + \sum_{j \in \mathcal{N}_t} e^{o_j} \right)} \\ &\stackrel{(i)}{\geq} \nabla_{\boldsymbol{\theta}} \mathcal{L} - \frac{M}{m} \sum_{k \in \mathcal{N}_t} \frac{e^{o_k} \cdot \left| \sum_{j \in \mathcal{N}_t} e^{o_j} - \frac{e^{o_k}}{q_k} \right|}{\left(e^{o_t} + \frac{m-1}{m} \cdot \sum_{j \in \mathcal{N}_t} e^{o_j} \right) \left(e^{o_t} + \sum_{j \in \mathcal{N}_t} e^{o_j} \right)} \cdot \mathbf{1} \\ &= \nabla_{\boldsymbol{\theta}} \mathcal{L} - \frac{M}{m} \sum_{k \in \mathcal{N}_t} \frac{e^{o_k} \cdot \left| \sum_{j \in \mathcal{N}_t} e^{o_j} - \frac{e^{o_k}}{q_k} \right|}{\left(e^{o_t} + \sum_{j \in \mathcal{N}_t} e^{o_j} \right)^2} \left(1 - o\left(\frac{1}{m}\right) \right) \cdot \mathbf{1} \end{aligned}$$

$$= \nabla_{\boldsymbol{\theta}} \mathcal{L} - \frac{M}{m} \sum_{k \in \mathcal{N}_t} \frac{e^{o_k} \cdot \left| \sum_{j \in \mathcal{N}_t} e^{o_j} - \frac{e^{o_k}}{q_k} \right|}{Z^2} \left(1 - o\left(\frac{1}{m}\right) \right) \cdot \mathbf{1}, \quad (22)$$

where (i) follows from the bound on the entries of $\nabla_{\boldsymbol{\theta}} o_k$, for each $k \in [n]$.

Upper bound: Using (18) and the upper bound in Lemma 1, we obtain that

$$\mathbb{E} [\nabla_{\boldsymbol{\theta}} \mathcal{L}'] \leq -\nabla_{\boldsymbol{\theta}} o_t + \mathbb{E}[U] \cdot \mathbb{E} \left[\frac{1}{V} \right] + \Delta_m, \quad (23)$$

where

$$\Delta_m \triangleq \frac{1}{m} \mathbb{E} \left[\sum_{k \in \mathcal{N}_t} \frac{e^{o_k} |\nabla_{\boldsymbol{\theta}} o_k| \cdot \left| \frac{e^{o_{sm}}}{q_{sm}} - \frac{e^{o_k}}{q_k} \right|}{\left(e^{o_t} + \sum_{i \in [m-1]} \frac{e^{o_{s_i}}}{mq_{s_i}} \right)^2} \right].$$

By employing Lemma 4 with (23), we obtain the following.

$$\begin{aligned} \mathbb{E} [\nabla_{\boldsymbol{\theta}} \mathcal{L}'] &\leq -\nabla_{\boldsymbol{\theta}} o_t + \frac{\mathbb{E}[U]}{\mathbb{E}[V]} + \mathbb{E}[U] \cdot \left(\frac{\sum_{j \in \mathcal{N}_t} \frac{e^{2o_j}}{q_j} - \left(\sum_{j \in \mathcal{N}_t} e^{o_j} \right)^2}{mZ^3} + o\left(\frac{1}{m}\right) \right) + \Delta_m \\ &= \nabla_{\boldsymbol{\theta}} \mathcal{L} + \mathbb{E}[U] \cdot \left(\frac{\sum_{j \in \mathcal{N}_t} \frac{e^{2o_j}}{q_j} - \left(\sum_{j \in \mathcal{N}_t} e^{o_j} \right)^2}{mZ^3} + o\left(\frac{1}{m}\right) \right) + \Delta_m \end{aligned} \quad (24)$$

By employing Lemma 2 in (24), we obtain that

$$\begin{aligned} \mathbb{E} [\nabla_{\boldsymbol{\theta}} \mathcal{L}'] &\leq \nabla_{\boldsymbol{\theta}} \mathcal{L} + \mathbb{E}[U] \cdot \left(\frac{\sum_{j \in \mathcal{N}_t} \frac{e^{2o_j}}{q_j} - \left(\sum_{j \in \mathcal{N}_t} e^{o_j} \right)^2}{mZ^3} + o\left(\frac{1}{m}\right) \right) + \\ &\quad \left(\frac{2M \max_{i, i' \in \mathcal{N}_t} \left| \frac{e^{o_i}}{q_i} - \frac{e^{o_{i'}}}{q_{i'}} \right| \sum_{j \in \mathcal{N}_t} e^{o_j}}{Z^2 + \sum_{j \in \mathcal{N}_t} \frac{e^{2o_j}}{q_j}} + o\left(\frac{1}{m}\right) \right) \cdot \mathbf{1} \end{aligned}$$

Now, using $\mathbb{E}[U] = \sum_{j \in [n]} e^{o_j} \cdot \nabla_{\boldsymbol{\theta}} o_j$ gives the stated upper bound. \square

Lemma 1. Let $\mathcal{S} = \{s_1, \dots, s_m\} \subset \mathcal{N}_t^m$ be m i.i.d. negative classes drawn according to the sampling distribution q . Then, the ratio appearing in the gradient estimate based on the sample softmax approach (cf. (8)) satisfies

$$\begin{aligned} \frac{e^{o_t} \cdot \nabla_{\boldsymbol{\theta}} o_t}{\sum_{j \in [n]} e^{o_j}} + \sum_{k \in \mathcal{N}_t} \frac{e^{o_k} \cdot \nabla_{\boldsymbol{\theta}} o_k}{e^{o_t} + \frac{m-1}{m} \cdot \sum_{j \in \mathcal{N}_t} e^{o_j} + \frac{e^{o_k}}{mq_k}} &\leq \\ \mathbb{E} \left[\frac{e^{o_t} \cdot \nabla_{\boldsymbol{\theta}} o_t + \sum_{i \in [m]} \left(\frac{e^{o_{s_i}}}{mq_{s_i}} \cdot \nabla_{\boldsymbol{\theta}} o_s \right)}{e^{o_t} + \sum_{i \in [m]} \frac{e^{o_{s_i}}}{mq_{s_i}}} \right] &\leq \\ \left(\sum_{k \in [n]} e^{o_k} \cdot \nabla_{\boldsymbol{\theta}} o_k \right) \cdot \mathbb{E} \left[\frac{1}{e^{o_t} + \sum_{i \in [m]} \frac{e^{o_{s_i}}}{mq_{s_i}}} \right] + \Delta_m, \end{aligned} \quad (25)$$

where

$$\Delta_m \triangleq \frac{1}{m} \mathbb{E} \left[\sum_{k \in \mathcal{N}_t} \frac{e^{o_k} |\nabla_{\boldsymbol{\theta}} o_k| \cdot \left| \frac{e^{o_{sm}}}{q_{sm}} - \frac{e^{o_k}}{q_k} \right|}{\left(e^{o_t} + \sum_{i \in [m-1]} \frac{e^{o_{s_i}}}{mq_{s_i}} \right)^2} \right] \quad (26)$$

Proof. Note that

$$\begin{aligned}
& \mathbb{E} \left[\frac{e^{o_t} \cdot \nabla_{\theta} o_t + \sum_{i \in [m]} \left(\frac{e^{o_{s_i}}}{mq_{s_i}} \cdot \nabla_{\theta} o_s \right)}{e^{o_t} + \sum_{i \in [m]} \frac{e^{o_{s_i}}}{mq_{s_i}}} \right] \\
&= \mathbb{E} \left[\frac{e^{o_t} \cdot \nabla_{\theta} o_t}{e^{o_t} + \sum_{j \in [m]} \frac{e^{o_{s_j}}}{mq_{s_j}}} \right] + \sum_{i \in [m]} \mathbb{E} \left[\frac{\left(\frac{e^{o_{s_i}}}{mq_{s_i}} \cdot \nabla_{\theta} o_{s_i} \right)}{e^{o_t} + \sum_{j \in [m]} \frac{e^{o_{s_j}}}{mq_{s_j}}} \right] \\
&= \mathbb{E} \left[\frac{e^{o_t} \cdot \nabla_{\theta} o_t}{e^{o_t} + \sum_{j \in [m]} \frac{e^{o_{s_j}}}{mq_{s_j}}} \right] + m \cdot \underbrace{\mathbb{E} \left[\frac{\left(\frac{e^{o_{s_m}}}{mq_{s_m}} \cdot \nabla_{\theta} o_{s_m} \right)}{e^{o_t} + \sum_{j \in [m]} \frac{e^{o_{s_j}}}{mq_{s_j}}} \right]}_{\text{Term I}} \tag{27}
\end{aligned}$$

For $1 \leq l \leq m$, let's define the notation $S_l \triangleq \sum_{j \in [l]} \frac{e^{o_j}}{q_j}$. Now, let's consider Term I.

$$\begin{aligned}
\text{Term I} &= \mathbb{E} \left[\mathbb{E} \left[\frac{\frac{e^{o_{s_m}}}{mq_{s_m}} \cdot \nabla_{\theta} o_{s_m}}{e^{o_t} + \frac{S_{m-1}}{m} + \frac{e^{o_{s_m}}}{mq_{s_m}}} \middle| S_{m-1} \right] \right] \\
&= \mathbb{E} \left[\sum_{k \in \mathcal{N}_t} q_k \cdot \frac{\frac{e^{o_k}}{mq_k} \cdot \nabla_{\theta} o_k}{e^{o_t} + \frac{S_{m-1}}{m} + \frac{e^{o_k}}{mq_k}} \right] \\
&= \frac{1}{m} \sum_{k \in \mathcal{N}_t} \mathbb{E} \left[\frac{e^{o_k} \cdot \nabla_{\theta} o_k}{e^{o_t} + \frac{S_{m-1}}{m} + \frac{e^{o_k}}{mq_k}} \right] \tag{28}
\end{aligned}$$

$$= \frac{1}{m} \sum_{k \in \mathcal{N}_t} \mathbb{E} \left[\frac{e^{o_k} \cdot \nabla_{\theta} o_k}{e^{o_t} + \frac{S_{m-1}}{m} + \frac{e^{o_k}}{mq_k}} - \frac{e^{o_k} \cdot \nabla_{\theta} o_k}{e^{o_t} + \frac{S_m}{m}} + \frac{e^{o_k} \cdot \nabla_{\theta} o_k}{e^{o_t} + \frac{S_m}{m}} \right] \tag{29}$$

$$\begin{aligned}
&= \frac{1}{m} \sum_{k \in \mathcal{N}_t} \mathbb{E} \left[\frac{e^{o_k} \cdot \nabla_{\theta} o_k}{e^{o_t} + \frac{S_{m-1}}{m} + \frac{e^{o_k}}{mq_k}} - \frac{e^{o_k} \cdot \nabla_{\theta} o_k}{e^{o_t} + \frac{S_m}{m}} \right] + \frac{1}{m} \sum_{k \in \mathcal{N}_t} e^{o_k} \cdot \nabla_{\theta} o_k \cdot \mathbb{E} \left[\frac{1}{e^{o_t} + \frac{S_m}{m}} \right] \\
&\leq \frac{1}{m^2} \mathbb{E} \left[\sum_{k \in \mathcal{N}_t} \frac{e^{o_k} |\nabla_{\theta} o_k| \cdot \left| \frac{e^{o_{s_m}}}{q_{s_m}} - \frac{e^{o_k}}{q_k} \right|}{\left(e^{o_t} + \frac{S_{m-1}}{m} + \frac{e^{o_k}}{mq_k} \right) \left(e^{o_t} + \frac{S_m}{m} \right)} \right] + \frac{1}{m} \sum_{k \in \mathcal{N}_t} e^{o_k} \cdot \nabla_{\theta} o_k \cdot \mathbb{E} \left[\frac{1}{e^{o_t} + \frac{S_m}{m}} \right] \\
&\stackrel{(i)}{\leq} \frac{1}{m^2} \mathbb{E} \left[\sum_{k \in \mathcal{N}_t} \frac{e^{o_k} |\nabla_{\theta} o_k| \cdot \left| \frac{e^{o_{s_m}}}{q_{s_m}} - \frac{e^{o_k}}{q_k} \right|}{\left(e^{o_t} + \frac{S_{m-1}}{m} \right)^2} \right] + \frac{1}{m} \sum_{k \in \mathcal{N}_t} e^{o_k} \cdot \nabla_{\theta} o_k \cdot \mathbb{E} \left[\frac{1}{e^{o_t} + \frac{S_m}{m}} \right], \tag{30}
\end{aligned}$$

where (i) follows by dropping the positive terms $\frac{e^{o_k}}{mq_k}$ and $\frac{e^{o_{s_i}}}{mq_{s_i}}$. Next, we combine (27) and (30) to obtain the following.

$$\begin{aligned}
& \mathbb{E} \left[\frac{e^{o_t} \cdot \nabla_{\theta} o_t + \sum_{i \in [m]} \left(\frac{e^{o_{s_i}}}{mq_{s_i}} \cdot \nabla_{\theta} o_s \right)}{e^{o_t} + \sum_{i \in [m]} \frac{e^{o_{s_i}}}{mq_{s_i}}} \right] \\
&\leq e^{o_t} \cdot \nabla_{\theta} o_t \cdot \mathbb{E} \left[\frac{1}{e^{o_t} + \frac{S_m}{m}} \right] + \sum_{k \in \mathcal{N}_t} e^{o_k} \cdot \nabla_{\theta} o_k \cdot \mathbb{E} \left[\frac{1}{e^{o_t} + \frac{S_m}{m}} \right] + \\
&\quad \frac{1}{m} \mathbb{E} \left[\sum_{k \in \mathcal{N}_t} \frac{e^{o_k} |\nabla_{\theta} o_k| \cdot \left| \frac{e^{o_{s_m}}}{q_{s_m}} - \frac{e^{o_k}}{q_k} \right|}{\left(e^{o_t} + \frac{S_{m-1}}{m} \right)^2} \right]
\end{aligned}$$

$$\begin{aligned}
&= \left(\sum_{k \in [n]} e^{o_k} \cdot \nabla_{\boldsymbol{\theta}} o_k \right) \cdot \mathbb{E} \left[\frac{1}{e^{o_t} + \sum_{i \in [m]} \frac{e^{o_{s_i}}}{mq_{s_i}}} \right] + \frac{1}{m} \mathbb{E} \left[\sum_{k \in \mathcal{N}_t} \frac{e^{o_k} |\nabla_{\boldsymbol{\theta}} o_k| \cdot \left| \frac{e^{o_{sm}}}{q_{sm}} - \frac{e^{o_k}}{q_k} \right|}{\left(e^{o_t} + \frac{S_{m-1}}{m} \right)^2} \right] \\
&= \left(\sum_{k \in [n]} e^{o_k} \cdot \nabla_{\boldsymbol{\theta}} o_k \right) \cdot \mathbb{E} \left[\frac{1}{e^{o_t} + \sum_{i \in [m]} \frac{e^{o_{s_i}}}{mq_{s_i}}} \right] + \Delta_m. \tag{31}
\end{aligned}$$

This completes the proof of the upper bound in (25). In order to establish the lower bound in (25), we combine (27) and (28) to obtain that

$$\begin{aligned}
&\mathbb{E} \left[\frac{e^{o_t} \cdot \nabla_{\boldsymbol{\theta}} o_t + \sum_{i \in [m]} \left(\frac{e^{o_{s_i}}}{mq_{s_i}} \cdot \nabla_{\boldsymbol{\theta}} o_{s_i} \right)}{e^{o_t} + \sum_{i \in [m]} \frac{e^{o_{s_i}}}{mq_{s_i}}} \right] \\
&= \mathbb{E} \left[\frac{e^{o_t} \cdot \nabla_{\boldsymbol{\theta}} o_t}{e^{o_t} + \sum_{j \in [m]} \frac{e^{o_{s_j}}}{mq_{s_j}}} \right] + \sum_{k \in \mathcal{N}_t} \mathbb{E} \left[\frac{e^{o_k} \cdot \nabla_{\boldsymbol{\theta}} o_k}{e^{o_t} + \frac{S_{m-1}}{m} + \frac{e^{o_k}}{mq_k}} \right] \\
&\geq \frac{e^{o_t} \cdot \nabla_{\boldsymbol{\theta}} o_t}{\sum_{j \in [n]} e^{o_j}} + \sum_{k \in \mathcal{N}_t} \frac{e^{o_k} \cdot \nabla_{\boldsymbol{\theta}} o_k}{e^{o_t} + \frac{m-1}{m} \cdot \sum_{j \in \mathcal{N}_t} e^{o_j} + \frac{e^{o_k}}{mq_k}}, \tag{32}
\end{aligned}$$

where the final step follows by applying Jensen's inequality to each of the expectation terms. \square

Lemma 2. For any model parameter $\boldsymbol{\theta} \in \Theta$, assume that we have the following bound on the maximum absolute value of each of coordinates of the gradient vectors

$$\|\nabla_{\boldsymbol{\theta}} o_j\|_{\infty} \leq M \quad \forall j \in [n]. \tag{33}$$

Then, Δ_m defined in Lemma 1 satisfies

$$\begin{aligned}
\Delta_m &\triangleq \frac{1}{m} \mathbb{E} \left[\sum_{k \in \mathcal{N}_t} \frac{e^{o_k} |\nabla_{\boldsymbol{\theta}} o_k| \cdot \left| \frac{e^{o_{sm}}}{q_{sm}} - \frac{e^{o_k}}{q_k} \right|}{\left(e^{o_t} + \sum_{i \in [m-1]} \frac{e^{o_{s_i}}}{mq_{s_i}} \right)^2} \right] \\
&\leq \left(\frac{2M \max_{i, i' \in \mathcal{N}_t} \left| \frac{e^{o_i}}{q_i} - \frac{e^{o_{i'}}}{q_{i'}} \right| \sum_{j \in \mathcal{N}_t} e^{o_j}}{Z^2 + \sum_{j \in \mathcal{N}_t} \frac{e^{2o_j}}{q_j}} + o\left(\frac{1}{m}\right) \right) \cdot \mathbf{1}, \tag{34}
\end{aligned}$$

where $\mathbf{1}$ is the all one vector.

Proof. Note that

$$\begin{aligned}
\Delta_m &\triangleq \frac{1}{m} \mathbb{E} \left[\sum_{k \in \mathcal{N}_t} \frac{e^{o_k} |\nabla_{\boldsymbol{\theta}} o_k| \cdot \left| \frac{e^{o_{sm}}}{q_{sm}} - \frac{e^{o_k}}{q_k} \right|}{\left(e^{o_t} + \sum_{i \in [m-1]} \frac{e^{o_{s_i}}}{mq_{s_i}} \right)^2} \right] \\
&\leq \frac{1}{m} \mathbb{E} \left[\sum_{k \in \mathcal{N}_t} \frac{e^{o_k} |\nabla_{\boldsymbol{\theta}} o_k| \cdot \max_{i, i' \in \mathcal{N}_t} \left| \frac{e^{o_i}}{q_i} - \frac{e^{o_{i'}}}{q_{i'}} \right|}{\left(e^{o_t} + \sum_{i \in [m-1]} \frac{e^{o_{s_i}}}{mq_{s_i}} \right)^2} \right] \\
&\leq \frac{2 \cdot \max_{i, i' \in \mathcal{N}_t} \left| \frac{e^{o_i}}{q_i} - \frac{e^{o_{i'}}}{q_{i'}} \right|}{m} \cdot \mathbb{E} \left[\frac{1}{\left(e^{o_t} + \frac{S_{m-1}}{m} \right)^2} \right] \cdot \sum_{k \in \mathcal{N}_t} e^{o_k} |\nabla_{\boldsymbol{\theta}} o_k|
\end{aligned}$$

$$\stackrel{(i)}{\leq} \frac{2M \cdot \max_{i,i' \in \mathcal{N}_t} \left| \frac{e^{o_i}}{q_i} - \frac{e^{o_{i'}}}{q_{i'}} \right|}{m} \cdot \mathbb{E} \left[\frac{1}{\left(e^{o_t} + \frac{S_{m-1}}{m} \right)^2} \right] \cdot \left(\sum_{k \in \mathcal{N}_t} e^{o_k} \right) \cdot \mathbf{1}, \quad (35)$$

where (i) follows from the fact that the gradients have bounded entries. Now, combining (35) and Lemma 3 gives us that

$$\Delta_m \leq \left(\frac{2M \max_{i,i' \in \mathcal{N}_t} \left| \frac{e^{o_i}}{q_i} - \frac{e^{o_{i'}}}{q_{i'}} \right| \sum_{j \in \mathcal{N}_t} e^{o_j}}{m \left(Z^2 + \sum_{j \in \mathcal{N}_t} \frac{e^{2o_j}}{q_j} \right)} + o\left(\frac{1}{m}\right) \right) \cdot \mathbf{1}. \quad (36)$$

□

Lemma 3. Consider the random variable

$$W = \left(e^{o_t} + \frac{S_{m-1}}{m} \right)^2. \quad (37)$$

Then, we have

$$\mathbb{E} \left[\frac{1}{W} \right] = \frac{1}{Z^2 + \sum_{j \in \mathcal{N}_t} \frac{e^{2o_j}}{q_j}} + \mathcal{O} \left(\frac{1}{m} \right). \quad (38)$$

Proof. Note that

$$\begin{aligned} \mathbb{E}[W] &= \mathbb{E} \left[\left(e^{o_t} + \frac{S_{m-1}}{m} \right)^2 \right] \\ &= e^{2o_t} + \frac{2e^{o_t}}{m} \sum_{i \in [m-1]} \mathbb{E} \left[\frac{e^{o_{s_i}}}{q_{s_i}} \right] + \frac{1}{m^2} \mathbb{E} \left[\sum_{i,i' \in [m-1]} \frac{e^{o_{s_i} + o_{s_{i'}}}}{q_{s_i} q_{s_{i'}}} \right] \\ &= e^{2o_t} + \frac{m-1}{m} \cdot 2e^{o_t} \sum_{j \in \mathcal{N}_t} e^{o_j} + \frac{1}{m^2} \mathbb{E} \left[\sum_{i,i' \in [m-1]} \frac{e^{o_{s_i} + o_{s_{i'}}}}{q_{s_i} q_{s_{i'}}} \right] \\ &= e^{2o_t} + \frac{m-1}{m} \cdot 2e^{o_t} \sum_{j \in \mathcal{N}_t} e^{o_j} + \frac{m-1}{m} \cdot \sum_{j \in \mathcal{N}_t} \frac{e^{2o_j}}{q_j} + \frac{(m-1)(m-2)}{m^2} \cdot \sum_{j,j' \in \mathcal{N}_t} e^{o_j + o_{j'}} \\ &= Z^2 + \sum_{j \in \mathcal{N}_t} \frac{e^{2o_j}}{q_j} - \frac{1}{m} \cdot 2e^{o_t} \sum_{j \in \mathcal{N}_t} e^{o_j} - \frac{1}{m} \cdot \sum_{j \in \mathcal{N}_t} \frac{e^{2o_j}}{q_j} - \frac{3m-2}{m^2} \cdot \sum_{j,j' \in \mathcal{N}_t} e^{o_j + o_{j'}} \\ &\triangleq \overline{W}_m. \end{aligned} \quad (39)$$

Furthermore, one can verify that $\text{Var}(W)$ scale as $\mathcal{O}\left(\frac{1}{m}\right)$. Therefore, using (56) in Lemma 5, we have

$$\mathbb{E} \left[\frac{1}{W} \right] \leq \frac{1}{\mathbb{E}[W]} + \frac{\text{Var}(W)}{e^{6o_t}} = \frac{1}{\mathbb{E}[W]} + \mathcal{O} \left(\frac{1}{m} \right). \quad (40)$$

Now, it follows from (39) and (40) that

$$\mathbb{E} \left[\frac{1}{W} \right] \leq \frac{1}{\overline{W}_m} + \mathcal{O} \left(\frac{1}{m} \right),$$

which with some additional algebra can be shown to be

$$\mathbb{E}\left[\frac{1}{W}\right] = \frac{1}{Z^2 + \sum_{j \in \mathcal{N}_t} \frac{e^{2o_j}}{q_j}} + \mathcal{O}\left(\frac{1}{m}\right).$$

□

Lemma 4. Consider the random variable

$$V = e^{ot} + \sum_{i \in [m]} \frac{e^{os_i}}{mq_{s_i}}. \quad (41)$$

Then, we have

$$\mathbb{E}\left[\frac{1}{V}\right] \leq \frac{1}{\mathbb{E}[V]} + \frac{\sum_{j \in \mathcal{N}_t} \frac{e^{2o_j}}{q_j} - \left(\sum_{j \in \mathcal{N}_t} e^{o_j}\right)^2}{mZ^3} + o\left(\frac{1}{m}\right). \quad (42)$$

Proof. We have from Lemma 5 that

$$\mathbb{E}\left[\frac{1}{V}\right] \leq \frac{1}{\mathbb{E}[V]} + \frac{\text{Var}(V)}{\mathbb{E}[V]^3} + o\left(\frac{1}{m}\right). \quad (43)$$

Note that

$$\begin{aligned} \mathbb{E}[V^2] &= e^{2ot} + \frac{e^{ot}}{m} \mathbb{E}\left[\sum_{i \in [m]} \frac{2e^{os_i}}{q_{s_i}}\right] + \frac{1}{m^2} \cdot \mathbb{E}\left[\sum_{i, i' \in [m]} \frac{e^{os_i + os_{i'}}}{q_{s_i} q_{s_{i'}}}\right] \\ &= e^{2ot} + 2e^{ot} \cdot \sum_{j \in \mathcal{N}_t} e^{o_j} + \frac{1}{m^2} \cdot \mathbb{E}\left[\sum_{i \in [m]} \frac{e^{2os_i}}{q_{s_i}^2} + \sum_{i \neq i' \in [m]} \frac{e^{os_i + os_{i'}}}{q_{s_i} q_{s_{i'}}}\right] \\ &= e^{2ot} + 2e^{ot} \cdot \sum_{j \in \mathcal{N}_t} e^{o_j} + \frac{1}{m} \cdot \sum_{j \in \mathcal{N}_t} \frac{e^{2o_j}}{q_j} + \frac{m-1}{m} \cdot \sum_{j, j' \in \mathcal{N}_t} e^{o_j + o_{j'}} \\ &= e^{2ot} + 2e^{ot} \cdot \sum_{j \in \mathcal{N}_t} e^{o_j} + \sum_{j, j' \in \mathcal{N}_t} e^{o_j + o_{j'}} + \frac{1}{m} \cdot \sum_{j \in \mathcal{N}_t} \frac{e^{2o_j}}{q_j} - \frac{1}{m} \cdot \sum_{j, j' \in \mathcal{N}_t} e^{o_j + o_{j'}} \\ &= \left(\sum_{j \in [n]} e^{o_j}\right)^2 + \frac{1}{m} \cdot \sum_{j \in \mathcal{N}_t} \frac{e^{2o_j}}{q_j} - \frac{1}{m} \cdot \sum_{j, j' \in \mathcal{N}_t} e^{o_j + o_{j'}} \\ &= \mathbb{E}[V]^2 + \frac{1}{m} \cdot \sum_{j \in \mathcal{N}_t} \frac{e^{2o_j}}{q_j} - \frac{1}{m} \cdot \sum_{j, j' \in \mathcal{N}_t} e^{o_j + o_{j'}} \end{aligned} \quad (44)$$

Therefore, we have

$$\text{Var}(V) = \mathbb{E}[V^2] - \mathbb{E}[V]^2 = \frac{1}{m} \cdot \sum_{j \in \mathcal{N}_t} \frac{e^{2o_j}}{q_j} - \frac{1}{m} \cdot \sum_{j, j' \in \mathcal{N}_t} e^{o_j + o_{j'}} \quad (45)$$

Now, by combining (43) and (45) we obtain that

$$\mathbb{E}\left[\frac{1}{V}\right] \leq \frac{1}{\mathbb{E}[V]} + \frac{\sum_{j \in \mathcal{N}_t} \frac{e^{2o_j}}{q_j} - \sum_{j, j' \in \mathcal{N}_t} e^{o_j + o_{j'}}}{mZ^3} + o\left(\frac{1}{m}\right)$$

$$= \frac{1}{\mathbb{E}[V]} + \frac{\sum_{j \in \mathcal{N}_t} \frac{e^{2\sigma_j}}{q_j} - \left(\sum_{j \in \mathcal{N}_t} e^{\sigma_j} \right)^2}{mZ^3} + o\left(\frac{1}{m}\right).$$

□

B Proof of Theorem 2

Proof. Recall that RFFs provide an unbiased estimate of the Gaussian kernel. Therefore, we have

$$\mathbb{E} \left[\phi_{\frac{1}{\sqrt{\nu}}, D}(\mathbf{c}_i)^T \phi_{\frac{1}{\sqrt{\nu}}, D}(\mathbf{h}) \right] = e^{-\nu \|\mathbf{c}_i - \mathbf{h}\|^2 / 2} = e^{-\nu} \cdot e^{\nu \mathbf{c}_i^T \mathbf{h}}. \quad (46)$$

In fact, for large enough D , the RFFs provide a tight approximation of $e^{-\nu} \cdot \exp(\nu \mathbf{c}_i^T \mathbf{h})$ [19, 23]. This follows from the observation that

$$\phi_{\frac{1}{\sqrt{\nu}}, D}(\mathbf{c}_i)^T \phi_{\frac{1}{\sqrt{\nu}}, D}(\mathbf{h}) = \frac{1}{\sqrt{D}} \sum_{j=1}^D \cos(\mathbf{w}_j^T (\mathbf{c}_i - \mathbf{h})) \quad (47)$$

is a sum of D bounded random variables

$$\left\{ \cos(\mathbf{w}_j^T (\mathbf{c}_i - \mathbf{h})) \right\}_{j \in [D]}.$$

Here, $\mathbf{w}_1, \dots, \mathbf{w}_D$ are i.i.d. random variable distributed according to the normal distribution $N(0, \nu \mathbf{I})$. Therefore, the following holds for all ℓ_2 -normalized vectors $\mathbf{u}, \mathbf{v} \in \mathbb{R}^d$ with probability at least $1 - \mathcal{O}\left(\frac{1}{D^2}\right)$ [19, 23].

$$\left| \phi_{\frac{1}{\sqrt{\nu}}, D}(\mathbf{u})^T \phi_{\frac{1}{\sqrt{\nu}}, D}(\mathbf{v}) - e^{-\nu} \cdot e^{\nu \mathbf{u}^T \mathbf{v}} \right| \leq \rho \sqrt{\frac{d}{D}} \log(D), \quad (48)$$

where $\rho > 0$ is a constant. Note that we have

$$q_i = \frac{\phi_{\frac{1}{\sqrt{\nu}}, D}(\mathbf{c}_i)^T \phi_{\frac{1}{\sqrt{\nu}}, D}(\mathbf{h})}{\sum_{j \in \mathcal{N}_t} \phi_{\frac{1}{\sqrt{\nu}}, D}(\mathbf{c}_j)^T \phi_{\frac{1}{\sqrt{\nu}}, D}(\mathbf{h})} = \frac{1}{C} \cdot \phi_{\frac{1}{\sqrt{\nu}}, D}(\mathbf{c}_i)^T \phi_{\frac{1}{\sqrt{\nu}}, D}(\mathbf{h}) \quad \forall i \in \mathcal{N}_t, \quad (49)$$

where the input embedding \mathbf{h} and the class embeddings $\mathbf{c}_1, \dots, \mathbf{c}_n$ are ℓ_2 -normalized. Therefore, it follows from (48) that the following holds with probability at least $1 - \mathcal{O}\left(\frac{1}{D^2}\right)$.

$$\frac{e^{\tau \mathbf{c}_i^T \mathbf{h}}}{e^{-\nu} e^{\nu \mathbf{c}_i^T \mathbf{h}} + \rho \sqrt{\frac{d}{D}} \log(D)} \leq \frac{1}{C} \cdot \left| \frac{e^{o_i}}{q_i} \right| \leq \frac{e^{\tau \mathbf{c}_i^T \mathbf{h}}}{e^{-\nu} e^{\nu \mathbf{c}_i^T \mathbf{h}} - \rho \sqrt{\frac{d}{D}} \log(D)}$$

or

$$\frac{e^{(\tau - \nu) \mathbf{c}_i^T \mathbf{h}}}{1 + \rho \sqrt{\frac{d}{D}} \log(D) \cdot e^{\nu(1 - \mathbf{c}_i^T \mathbf{h})}} \leq \frac{1}{C e^{\nu}} \cdot \left| \frac{e^{o_i}}{q_i} \right| \leq \frac{e^{(\tau - \nu) \mathbf{c}_i^T \mathbf{h}}}{1 - \rho \sqrt{\frac{d}{D}} \log(D) \cdot e^{\nu(1 - \mathbf{c}_i^T \mathbf{h})}}. \quad (50)$$

Since we assume that both the input and the class embedding are normalize, we have

$$\exp(\nu \mathbf{c}_i^T \mathbf{h}) \in [e^{-\nu}, e^{\nu}]. \quad (51)$$

Thus, as long as, we ensure that

$$\rho\sqrt{\frac{d}{D}}\log(D)\cdot e^{2\nu}\leq\gamma_1\text{ or }e^{2\nu}\leq\frac{\gamma_1}{\rho\sqrt{d}}\cdot\frac{\sqrt{D}}{\log D}\quad(52)$$

for a small enough constant γ , it follows from (50) that

$$\frac{e^{(\tau-\nu)\mathbf{c}_i^T\mathbf{h}}}{1+\gamma_1}\leq\frac{1}{Ce^\nu}\cdot\left|\frac{e^{o_i}}{q_i}\right|\leq\frac{e^{(\tau-\nu)\mathbf{c}_i^T\mathbf{h}}}{1-\gamma_1}.\quad(53)$$

or

$$e^{(\tau-\nu)\mathbf{c}_i^T\mathbf{h}}\cdot(1-\gamma'_1)\leq\frac{1}{Ce^\nu}\cdot\left|\frac{e^{o_i}}{q_i}\right|\leq e^{(\tau-\nu)\mathbf{c}_i^T\mathbf{h}}\cdot(1+\gamma'_1),\quad(54)$$

where $\gamma'_1 > 0$ is a constant that depends of γ_1 . Using the similar arguments, it also follows from (48) that with probability at least $1 - \mathcal{O}\left(\frac{1}{D^2}\right)$, we have

$$(1-\gamma_1)\cdot e^{-\nu}\cdot\sum_{i\in\mathcal{N}_t}e^{o_i}\leq C\leq(1+\gamma_1)\cdot e^{-\nu}\cdot\sum_{i\in\mathcal{N}_t}e^{o_i}\quad(55)$$

Now, by combining (54) and (55), we get that

$$e^{(\tau-\nu)\mathbf{c}_i^T\mathbf{h}}\cdot(1-\gamma_2)\leq\frac{1}{\sum_{i\in\mathcal{N}_t}e^{o_i}}\cdot\left|\frac{e^{o_i}}{q_i}\right|\leq e^{(\tau-\nu)\mathbf{c}_i^T\mathbf{h}}\cdot(1+\gamma_2),$$

where γ_2 is constant depending on γ_1 . □

C Toolbox

Lemma 5. *For a positive random variable V such that $V \geq a > 0$, its expectation satisfies the following.*

$$\frac{1}{\mathbb{E}[V]}\leq\mathbb{E}\left[\frac{1}{V}\right]\leq\frac{1}{\mathbb{E}[V]}+\frac{\text{Var}(V)}{a^3}.\quad(56)$$

and

$$\frac{1}{\mathbb{E}[V]}\leq\mathbb{E}\left[\frac{1}{V}\right]\leq\frac{1}{\mathbb{E}[V]}+\frac{\text{Var}(V)}{\mathbb{E}[V]^3}+\frac{\mathbb{E}|V-\mathbb{E}[V]|^3}{a^4}.\quad(57)$$

Proof. It follows from the Jensen's inequality that

$$\mathbb{E}\left[\frac{1}{V}\right]\geq\frac{1}{\mathbb{E}[V]}.\quad(58)$$

For the upper bound in (56), note that the first order Taylor series expansion of the function $f(x) = \frac{1}{x}$ around $x = \mathbb{E}[V]$ gives us the following.

$$\frac{1}{x}=\frac{1}{\mathbb{E}[V]}-\frac{x-\mathbb{E}[V]}{\mathbb{E}[V]^2}+\frac{(x-\mathbb{E}[V])^2}{\xi^3},\quad(59)$$

where ξ is constant that falls between x and $\mathbb{E}[V]$. This gives us that

$$\begin{aligned}
\mathbb{E} \left[\frac{1}{V} \right] &\leq \frac{1}{\mathbb{E}[V]} - \frac{\mathbb{E}(V - \mathbb{E}[V])}{\mathbb{E}[V]^2} + \mathbb{E} \left[\frac{(V - \mathbb{E}[V])^2}{(\min\{V, \mathbb{E}[V]\})^3} \right] \\
&= \frac{1}{\mathbb{E}[V]} + \mathbb{E} \left[\frac{(V - \mathbb{E}[V])^2}{(\min\{V, \mathbb{E}[V]\})^3} \right] \\
&\stackrel{(i)}{\leq} \frac{1}{\mathbb{E}[V]} + \frac{\mathbb{E}[V - \mathbb{E}[V]]^2}{a^3} \\
&= \frac{1}{\mathbb{E}[V]} + \frac{\text{var}(V)}{a^3},
\end{aligned} \tag{60}$$

where (i) follows from the assumption that $V \geq a > 0$.

For the upper bound in (57), let's consider the second order Taylor series expansion for the function $f(x) = \frac{1}{x}$ around $\mathbb{E}[V]$.

$$\frac{1}{x} = \frac{1}{\mathbb{E}[V]} - \frac{x - \mathbb{E}[V]}{\mathbb{E}[V]^2} + \frac{(x - \mathbb{E}[V])^2}{\mathbb{E}[V]^3} - \frac{(x - \mathbb{E}[V])^3}{\chi^4}, \tag{61}$$

where χ is a constant between x and $\mathbb{E}[V]$. Note that the final term in the right hand side of (61) can be bounded as

$$\frac{(x - \mathbb{E}[V])^3}{\chi^4} \geq \frac{(x - \mathbb{E}[V])^3}{x^4}. \tag{62}$$

Combining (56) and (62) give us that

$$\frac{1}{x} \leq \frac{1}{\mathbb{E}[V]} - \frac{x - \mathbb{E}[V]}{\mathbb{E}[V]^2} + \frac{(x - \mathbb{E}[V])^2}{\mathbb{E}[V]^3} - \frac{(x - \mathbb{E}[V])^3}{x^4}. \tag{63}$$

It follows from (63) that

$$\begin{aligned}
\mathbb{E} \left[\frac{1}{V} \right] &\leq \frac{1}{\mathbb{E}[V]} + \frac{\text{Var}(V)}{\mathbb{E}[V]^3} + \mathbb{E} \left[\frac{|V - \mathbb{E}[V]|^3}{V^4} \right] \\
&\leq \frac{1}{\mathbb{E}[V]} + \frac{\text{Var}(V)}{\mathbb{E}[V]^3} + \frac{\mathbb{E} \left[|V - \mathbb{E}[V]|^3 \right]}{a^4}.
\end{aligned} \tag{64}$$

□